ORIGINAL RESEARCH

Growth Hormone–Releasing Hormone Agonists Reduce Myocardial Infarct Scar in Swine With Subacute Ischemic Cardiomyopathy

Luiza L. Bagno, DVM, PhD; Rosemeire M. Kanashiro-Takeuchi, DVM, PhD; Viky Y. Suncion, MD; Samuel Golpanian, MD; Vasileios Karantalis, MD; Ariel Wolf, BA; Bo Wang, MD; Courtney Premer, BS; Wayne Balkan, PhD; Jose Rodriguez, RTR, MR; David Valdes, BA; Marcos Rosado, AA; Norman L. Block, MD; Peter Goldstein, MS; Azorides Morales, MD; Ren-Zhi Cai, PhD; Wei Sha, BA; Andrew V. Schally, PhD, MD(hc), DSc(hc); Joshua M. Hare, MD

***Background*—**Growth hormone–releasing hormone agonists (GHRH-As) stimulate cardiac repair following myocardial infarction (MI) in rats through the activation of the GHRH signaling pathway within the heart. We tested the hypothesis that the administration of GHRH-As prevents ventricular remodeling in a swine subacute MI model.

***Methods and Results*—**Twelve female Yorkshire swine (25 to 30 kg) underwent transient occlusion of the left anterior descending coronary artery (MI). Two weeks post MI, swine were randomized to receive injections of either 30 μg/kg GHRH-A (MR-409) (GHRH-A group; n=6) or vehicle (placebo group; n=6). Cardiac magnetic resonance imaging and pressure–volume loops were obtained at multiple time points. Infarct, border, and remote (noninfarcted) zones were assessed for GHRH receptor by immunohistochemistry. Four weeks of GHRH-A treatment resulted in reduced scar mass (GHRH-A: −21.9±6.42%; *P*=0.02; placebo: 10.9±5.88%; *P*=0.25; 2-way ANOVA; *P*=0.003), and scar size (percentage of left ventricular mass) (GHRH-A: −38.38±4.63; *P*=0.0002; placebo: −14.56±6.92; *P*=0.16; 2-way ANOVA; *P*=0.02). This was accompanied by improved diastolic strain. Unlike in rats, this reduced infarct size in swine was not accompanied by improved cardiac function as measured by serial hemodynamic pressure–volume analysis. GHRH receptors were abundant in cardiac tissue, with a greater density in the border zone of the GHRH-A group compared with the placebo group.

***Conclusions*—**Daily subcutaneous administration of GHRH-A is feasible and safe in a large animal model of subacute ischemic cardiomyopathy. Furthermore, GHRH-A therapy significantly reduced infarct size and improved diastolic strain, suggesting a local activation of the GHRH pathway leading to the reparative process. **(*J Am Heart Assoc*. 2015;4:e001464 doi: 10.1161/JAHA.114.001464)**

Key Words: diastolic function • growth hormone–releasing hormone • heart failure • myocardial infarction • remodeling

Heart failure (HF) represents the major sequela of myocardial infarction (MI). This syndrome increases in prevalence with age and affects almost 10% of men and 8% of women over the age of 60.[1] Although the survival after HF has improved, mortality remains high—approximately 50% of people diagnosed with HF will die within 5 years.[1,2] Recent evidence indicates that growth hormone (GH) deficiency plays a crucial role in the functional abnormalities, disease progression, and mortality in HF patients.[3] Currently, a variety of new treatment strategies, including cellular,[4–6] pharmacological,[7] and genetic[7] treatments, have been developed for ischemic cardiomyopathy. These treatment modalities, including hormone therapy, focus on the regeneration or repair of damaged myocardium and restoration of cardiac function.[8–11]

Administration of GH-releasing hormone (GHRH) exerts important cardioprotection in the setting of ischemia–reperfusion injury in rats.[11] The administration of GHRH offers a highly physiological approach to treating cardiac injury based on its direct effect on cardiomyocyte and cardiac stem cell (CSC) receptors.[8,9,11,12] Although GHRH administration can potentially activate the GH/insulin-like growth factor (IGF)-1

From the Interdisciplinary Stem Cell Institute (L.L.B., R.M.K.-T., V.Y.S., S.G., V.K., A.W., B.W., C.P., W.B., J.R., D.V., M.R., J.M.H.), and Departments of Medicine (N.L.B., A.M., R.-Z.C., W.S., A.V.S., J.M.H.) and Molecular and Cellular Pharmacology (R.M.K.-T., C.P., J.M.H.), University of Miami Miller School of Medicine, Miami, FL; Bruce A. Carter Miami Veterans Affairs Healthcare System, Miami, FL (N.L.B., R.-Z.C., W.S., A.V.S.); Biscayne Pharmaceuticals Inc, Miami, FL (P.G.).

Correspondence to: Joshua M. Hare, MD, Interdisciplinary Stem Cell Institute, Biomedical Research Building, 1501 NW 10th Ave, Room 910, PO Box 016960 (R125), Miami, FL 33101. E-mail: jhare@med.miami.edu

Received September 23, 2014; accepted February 5, 2015.

axis, its ability to act independently of this axis can avoid the side effects associated with GH or IGF-1.[13,14] There are several clinical studies using GH replacement therapy for HF, but results are controversial.[10,15,16]

A synthetic analog of the human GHRH, GHRH agonist (GHRH-A), has demonstrated high activity and greater metabolic stability.[17] In previous studies, we showed a significant response to GHRH-A in acute and chronic ischemic injuries in rodent models. The GHRH-A (JI-38) stimulated substantial cardiac repair,[8] reversed ventricular remodeling,[9] and improved cardiac function.[8,9] Similar effects were obtained with a new series of GHRH-As, represented by MR-409.[18] Moreover, in rats, the GHRH-A did not alter circulating levels of GH and IGF-1, suggesting a direct cardiac effect.[8,9] To translationally advance the potential application of GHRH agonist to treat humans with post-MI remodeling, we tested the hypothesis that the GHRH-A MR-409 would exert cardioprotection in a model of infarct remodeling in the swine. Accordingly, we administered GHRH-A (MR-409) to Yorkshire pigs with subacute ischemic cardiomyopathy and tested the hypothesis that daily subcutaneous administration of GHRH-A for 4 weeks results in prevention and/or reversal of ventricular remodeling.

Materials and Methods

Animals and Study Design

All animal protocols were reviewed and approved by the University of Miami Institutional Animal Care and Use Committee. Twelve female Yorkshire swine (25 to 30 kg) were used in this double-blinded, randomized, placebo-controlled translational study. The MI in the swine model was induced via full occlusion of the left anterior descending coronary artery (LAD) by using balloon catheter inflation for 90 minutes.[19] Animals were randomized to receive injections of either GHRH-A—MR409 (GHRH-A; n=6) (structure: [*N*-Me-Tyr^{1}, D-Ala^{2}, Orn^{12}, Abu^{15}, Orn^{21}, Nle^{27}, Asp^{28}] hGH-RH$^{1-29}$, NH-CH_3, as previously reported[18]) or vehicle (placebo; n=6). Each study animal underwent noninvasive magnetic resonance imaging (MRI) and invasive hemodynamic assessment. Animals also underwent serial measurements of cardiac function and blood work as outlined in Table 1. All study procedures and analyses were performed by blinded investigators.

MI Induction

All animals in this study underwent closed-chest ischemic reperfusion MI as previously described,[19] in which MI was induced by the inflation of a coronary angioplasty balloon in the mid LAD. Access was obtained via a right carotid artery cutdown. The right internal carotid artery and external jugular vein were exposed and catheterized with 7-Fr and 10-Fr sheaths, respectively. Animals received heparin (100 to 200 IU/kg) before the start of occlusion. Lidocaine (2 to 4 mg/kg bolus followed by continuous infusion of 50 μg kg^{-1} min^{-1}) was administered to the animal. Coronary angiograms were obtained by fluoroscopy. Then, a 0.014-inch coronary guidewire was advanced into the LAD. A coronary angioplasty balloon (Cordis Fire Star) sized to match the diameter of the mid LAD (3.0×15 mm to 3.75×20 mm) was delivered to that segment and inflated distal to the first LAD diagonal branch, at the lowest pressure necessary to occlude distal flow. After 90 minutes, the balloon was deflated and removed to allow for reperfusion. The right carotid arteriotomy was repaired (if feasible) with 6-0 Prolene or ligated, and the external jugular vein was ligated. The surgical incision was closed in layers and sterilely dressed. Postprocedural pain was managed with buprenorphine (0.003 mg/kg) and transdermal fentanyl (25 to 75 μg kg^{-1} h^{-1}) for 72 hours. The swine was then recovered, and the myocardium was allowed to heal for 2 weeks.

Randomization

Randomization was conducted after the induction of MI.

Table 1. Experimental Time Points

Time Point	Baseline (MI)	Immediately Post MI	2 Weeks Post MI	Immediately Posttreatment	1 Week Posttreatment	2 Weeks Posttreatment	3 Weeks Posttreatment	4 Weeks Posttreatment
Treatment (start)			X					
Cardiac imaging	X		X			X		X
Pressure–volume loops	X		X					X
Death and necropsy								X
Blood work	X	X	X	X	X	X	X	X
Body weight	X		X		X	X	X	X

MI indicates myocardial infarction.

Table 2. Blood Sample Parameters

1. White blood cell count	12. Eosinophils	22. BUN	33. A/G ratio
2. Red blood cell count	13. Basophils	23. Crea	34. ALT
3. Hemoglobin	14. NRBC	24. BUN/Crea ratio	35. LDH
4. Hematocrit	15. RBC morphology	25. Sodium	36. CPK
5. MCV	16. Platelet morphology	26. Potassium	37. Alkaline phosphatase
6. MCH	17. WBC morphology	27. Calcium	38. Total bilirubin
7. MCHC	18. Platelet count	28. Magnesium	39. CK-MB (ortho)
8. Segmented neutrophils	19. Hemolysis index	29. Phosphorus	40. CK-MM
9. Band neutrophils	20. Lipemia index	30. Uric acid	41. CK-BB
10. Lymphocytes	21. Glucose	31. Total protein	42. Troponin-I, ng/mL
11. Monocytes		32. Albumin	43. GGT

A/G indicates albumin-to-globulin ratio; ALT, alanine transaminase; BUN, blood urea nitrogen; CK-BB, CK isoenzyme in brain; CK-MB, creatine kinase (CK) isoenzyme in heart; CK-MM, CK isoenzyme in skeletal muscle; CPK, creatine phosphokinase; Crea, creatinine; GGT, γ-glutamyl transferase; LDH, lactate dehydrogenase; MCV indicates mean corpuscular volume; MCH, mean corpuscular hemoglobin; MCHC, mean corpuscular hemoglobin concentration; NRBC, nucleated red blood cell; RBC, red blood cell; WBC, white blood cell.

Administration of GHRH-A

Animals were administered a daily subcutaneous injection of 30 μg/kg GHRH-A MR-409 or vehicle (dimethyl sulfoxide + propylene glycol) by blinded administrators. The treatment began 2 weeks post MI. Animals were weighed weekly, and the amount of drug to be administered was adjusted according to the animals' weight.

Blood Sample Analysis

Serum hematology, chemistry, and cardiac enzymes were measured at numerous time points throughout this study (see Table 1). Blood samples were obtained while the animal was under general anesthesia. EDTA-anticoagulated whole blood was collected for hematology; serum was collected for chemistry (clot tubes). All the measurements performed are summarized in Table 2.

Imaging

Cardiac magnetic resonance (CMR) imaging studies were conducted by using a Siemens Magnatom Trio, A Tim System (Erlangen, Germany) scanner with Syngo Numaris 4 (MR BV17A) software and an Invivo 16-channel Body Array Anterior Coil (Gainesville, FL) with retrospective gating and short breath-hold acquisitions. CMR was done to study the heart before MI (baseline), 2 weeks post MI (pretreatment), 2 weeks postadministration of the first dose of GHRH-A/vehicle (2 weeks posttreatment), and 4 weeks posttreatment (death).

Table 3. Swine Mass, Scar Mass, and Heart Weight (HW)/Body Weight (BW) Index Characteristics

	Baseline	2 Weeks Post MI (Pretreatment)	2 Weeks Posttreatment	4 Weeks Posttreatment
Swine mass, kg				
Placebo (n=6)	27.83±0.6	33.67±1.52	40.83±1.88	47.33±2.25
GHRH-A (n=6)	29.33±1.17	34.67±1.43	41±1.65	47.33±1.89
Scar mass, g				
Placebo (n=6)	—	8.13±0.96	—	—
GHRH-A (n=6)	—	9.04±1.03	—	—
Scar mass/LV mass				
Placebo (n=6)	—	13.45±1.35	—	—
GHRH-A (n=6)	—	13.71±1.21	—	—
HW/BW index				
Placebo (n=6)	—	5046.5±212.65	—	—
GHRH-A (n=6)	—	5587.2±398.74	—	—

GHRH-A indicates growth hormone–releasing hormone agonist; LV, left ventricular; MI, myocardial infarction.

Table 4. Average Values for Cardiac Enzymes (Troponin I, CK-MB, CK-MM, and CK-MB) by Treatment Group

Laboratory Test	Normal Values	Baseline (Pre MI)	Immediately Post MI	2 Weeks Post MI	Immediately Posttreatment	1 Week Posttreatment	2 Weeks Posttreatment	3 Weeks Posttreatment	4 Weeks Posttreatment
Placebo group									
Troponin-I	0.00 to 0.50	0.011	1.506	0.016	N/D	0.008	0.007	0.007	0.01
CK-MB		31.3	90.6	31.7	57.0	46.5	33.7	37.5	26.5
CK-MM		642.0	2992.2	721.5	2801.5	982.0	1272.7	1333.2	836.7
CK-MB		87.0	615.4	125.3	254.5	132.3	160.0	126.8	101.5
GHRH-A group									
Troponin-I	0.00 to 0.50	0.004	2.003	0.019	N/D	0.008	0.007	0.006	0.014
CK-MB		33.5	139.8	42.0	86.5	22.8	45.7	42.7	86.7
CK-MM		905.2	3424.7	1326.0	3596.0	653.3	1980.7	1654.7	2614.1
CK-MB		144.3	723.5	262.2	221.5	100.3	454.7	186.3	398.0

CK-BB indicates creatine kinase (CK) isoenzyme in brain; CK-MB, CK isoenzyme in heart; CK-MM, CK isoenzyme in skeletal muscle; GHRH-A, growth hormone–releasing hormone agonist; MI, myocardial infarction; N/D, no data.

Steady-state free precession cine images in 2-, 3-, and 4-chamber and short-axis planes (slice thickness 4 mm, field of view 280 to 300 mm, matrix 256×80, repetition time [TR] 43 ms, echo time [TE] 2.67 ms, number of averages 1, band width 441 Hz, flip angle 12°) were obtained. Two-chamber and short-axis planes were used for analyses. At end diastole and end systole, semiautomated epicardial and endocardial borders were drawn in contiguous short-axis cine images covering the apex–to–mitral valve plane by using Segment Software (Medviso AB) to calculate end-diastolic volume, end-systolic volume, and stroke volume.

Perfusion imaging was performed using injection boluses of Gd-DPTA. First-pass perfusion imaging was performed continuously for 1.5 minutes at rest immediately after an intravenous bolus injection of gadolinium (Gd-DPTA, 0.1 mmol/kg, 5 mL/s; Magnevist, Berlex, Wayne, NJ) with an ECG-gated interleaved saturation recovery gradient echo planar imaging pulse sequence. After completion of first-pass image acquisition, a second bolus of Gd-DTPA (0.1 mmol/kg) was injected. An entire short-axis stack was acquired every 2 to 4 heartbeats. Imaging parameters were as follows: TR/TE=162 and 0.94 ms; flip angle=10°; 128×128 matrix; 8-mm slice thickness/no gap; bandwidth 1002 Hz; 26-com field of view; and 1 number of average signals (NSA).

Short-axis and 2-, 3-, and 4-chamber long-axis delayed enhancement images (slice thickness of 4 mm with no gap, field of view 280 to 300 mm, matrix 256×100, TR/TE 567 ms/2.16 ms, band width 287 Hz, and a flip angle of 20°) were acquired 8 minutes following intravenous infusion of gadolinium 0.3 mmol/kg. Infarct scar size was calculated from the short-axis delayed myocardial enhancement images covering the apex–to–mitral valve plane (Kim et al[30]). By using Segment Software, epicardial and endocardial left ventricular (LV) contours were drawn with use of a semiautomated tool. The intensity of a normal region of myocardium was calculated, and scar tissue was determined by using an intensity threshold 2 SDs above normal myocardium.

Regional function was measured by tagged CMR images by using HARP software (Diagnosoft). Tagged MR images were collected in parallel planes throughout the short axis. Flash tagged images in the short-axis planes (slice thickness 8 mm, field of view 280 to 300 mm, matrix 256×80, TR 49 ms, TE 2.7 ms, number of averages 1, band width 446 Hz, flip angle 10°) were obtained. Three contiguous short-axis tagged images encompassing the scar were selected for analysis.

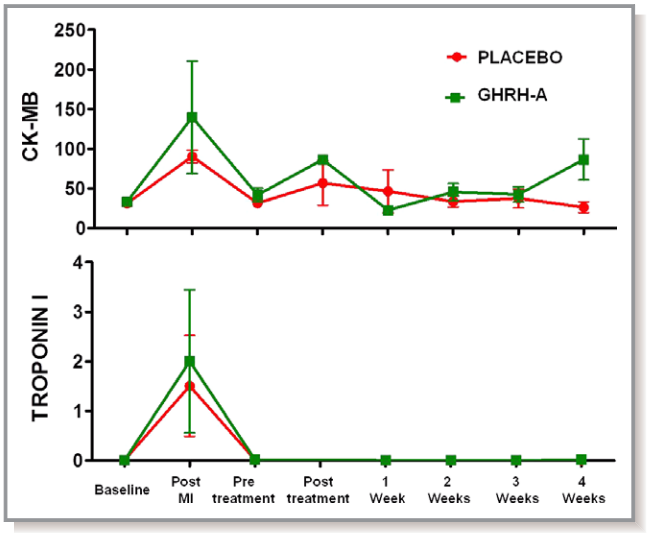

Figure 1. Average values for cardiac enzymes (CK-MB and troponin) in GHRH-A and placebo groups. GHRH-A indicates growth hormone–releasing hormone agonist.

Table 5. Hemodynamic Parameters

	Baseline	2 Weeks Post MI	4 Weeks Posttreatment
Integrated cardiac function			
SW (mm Hg×mL)/BSA (m^2)			
Placebo	2117±207.52	1568±133.64	2268±327.60
GHRH-A	2099±233.05	1850±176.66	2102±158.01
CO (L/min)/BSA (m^2)			
Placebo	4.00±0.164	3.32±0.091	4.39±0.433
GHRH-A	3.55±0.298	3.49±0.394	3.89±0.380
SV (mL)/BSA (m^2)			
Placebo	37.59±2.43	35.28±1.44	49.68±5.70*
GHRH-A	39.92±3.02	39.52±3.25	47.96±2.76
EF (%)			
Placebo	32.33±1.97	26.34±1.42	30.11±3.41
GHRH-A	34.84±2.53	31.28±2.97	29.89±2.82
Lusitropy			
EDPVR			
Placebo	0.19±0.03	0.17±0.03	0.17±0.03
GHRH-A	0.23±0.03	0.20±0.07	0.21±0.06
dP/dt min (mm Hg/s)			
Placebo	−1411±110.46	−889.74±113.68*	−1052±54.76
GHRH-A	−1429±108.88	−1171±96.15	−1076±135.24

N=5 or 6. BSA indicates body surface area; CO, cardiac output; EDPVR, end-diastolic pressure–volume relationship; EF, ejection fraction; GHRH-A, growth hormone–releasing hormone agonist; MI, myocardial infarction; SV, stroke volume; SW, stroke work.
One-way ANOVA within group: *P<0.05 vs baseline.

User-defined epicardial and endocardial contours were drawn to create a 24-segment mesh for each slice, and Eulerian circumferential strain for each segment at each time point of the cardiac cycle was measured. By using the right ventricular insertion as a reference point, corresponding tagged images were classified as either transmural infarction segments (scar ≥50% of the respective segment), margin of infarcted area (scar <50% of the respective segment), and remote area (remote segments to the infarction area). The peak Eulerian circumferential strain for each area was calculated by averaging the peak Eulerian circumferential strain (more negative is greater contractility) from each individual segment of the specified zone. The peak diastolic strain rate was calculated by averaging the most positive point in the early diastolic portion of the strain rate curve from each individual segment of the specified zone. The same slices and areas were used between all time points.

PV Analysis

Hemodynamic studies were scheduled to occur during the majority of procedures in accordance with Table 1. A pressure–volume (PV) loop transducer (Millar Instruments Inc) was zeroed and balanced in warm saline. The Millar catheter was inserted through the arterial vascular sheath into the LV, and baseline PV cardiac information was recorded. Then, a 3×20-mm balloon was inserted through the venous vascular sheath in the inferior vena cava to record occlusion PV cardiac information. The PV loop volumes were calibrated to corresponding CMR-derived end-diastolic volume and stroke volume by using the point-and-difference technique, which calibrates the conductance volume signal to the independently obtained CMR volume assessment.[19] Left ventricular PV loops were recorded at steady state and at varying preloads during temporary occlusion of the inferior vena cava. All analyses were performed by using LabChart 7 Pro software (AD Instruments Inc).

Necropsy and Histopathologic Analysis

At the end of the study, a necropsy was performed on each animal, and tissue samples of the brain, liver, spleen, kidney, lung, ileum, and pituitary gland were obtained and analyzed histologically for the presence of neoplastic tissue.

Table 6. Hemodynamic Parameters

	Baseline	2 Weeks Post MI	4 Weeks Posttreatment
Preload			
EDP, mmHg			
Placebo	17.71±2.37	17.05±3.95	18.67±2.57
GHRH-A	13.47±2.07	17.98±1.42	18.38±4.03
EDV (mL)/BSA (m^2)			
Placebo	117.54±1.90	138.34±6.24*	130.97±33.05*†
GHRH-A	116.54±4.75	132.42±5.87	165.94±10.06*†
Afterload			
Ea, mmHg/mL			
Placebo	3.18±0.22	2.60±0.33*	1.85±0.27
GHRH-A	2.83±0.21	2.57±0.18*	1.93±0.12
Contractility			
dP/dt max, mmHg/s			
Placebo	1161±88.21	946.06±82.96	1081±118.46
GHRH-A	1008±66.06	996.30±49.81	894.38±68.46
PRSW			
Placebo	26.48±3.30	16.68±4.17	38.73±6.06†
GHRH-A	30.52±2.69	25.87±1.88	33.13±4.27
ESPVR			
Placebo	1.45±0.10	1.06±0.20	1.27±0.17
GHRH-A	1.17±0.22	1.07±0.20	1.44±0.18

N=5 or 6. BSA indicates body surface area; Ea, arterial elastance; EDP, end-diastolic pressure; EDV, end-diastolic volume; ESPVR, end-systolic pressure–volume relationship; GHRH-A, growth hormone–releasing hormone agonist; MI, myocardial infarction; PRSW, preload recruitable stroke work.
One-way ANOVA within group: *P<0.05 vs baseline. †P<0.05 vs 2 weeks post MI.

Gross and Microscopic Histology of the Heart

At necropsy, the heart was harvested for analysis and a heart weight/body weight index determined. The LV was sliced into 10 rings along the short-axis plane of the ventricle. Both surfaces of these ventricular slices were photographed while immersed in water to eliminate highlights, and digital images were obtained. Samples of infarct, border, and remote (noninfarcted) zones were isolated and stored in formalin for histological analysis. Histochemical staining, including hematoxylin and eosin and Masson's trichrome as appropriate, was used to evaluate myocardial regeneration. GHRH receptor (GHRHR) expression was assessed by immunohistochemical staining in the cardiac tissue following GHRH-A or placebo treatment by using an anti-GHRHR antibody (rabbit polyclonal to GHRHR—ab28692 [Abcam]). The histology and immunohistochemical staining were performed on 3-μm-thick paraffin sections of tissues fixed in buffered formalin according to the manufacturer's protocol. All images were obtained by using a ×10 magnification, and the settings were constant for the entire study. All slides were analyzed and pictured in a digital microscope (VisionTek; Sakura). One image was taken from each sample (infarct, border, and remote zones) for histology and immunohistochemistry assays. Morphometric analyses for the hematoxylin and eosin/trichrome staining were performed by a blinded pathologist (qualitative analyses). The quantification of immunohistochemistry was performed following deconvolution (Image J software, version 1.44p; Wayne Rasband, National Institutes of Health), with no previous knowledge of the sample identification. A mean gray value of 3 distinct selected areas was generated by using the point tool, and the mean staining intensity (intensity/pixel) was recorded. The GHRHR expression was quantified by gray color intensity and is inversely correlated with GHRHR expression.

Vascular Density Assessment

Immunohistochemistry staining was performed with von Willebrand factor VIII antibody to calculate the vascular density. For the vascular density quantification, representative samples were selected from the border zone containing infarct and nonscarred tissue from the LV wall of all cardiac samples from

Table 7. Cine Image Analyses and Perfusion by CMR and Contractility Index by Tagging

	Baseline	2 Weeks Post MI	4 Weeks Posttreatment
Cine			
ESV, mL			
Placebo	48.88±1.73	71.67±5.92	88.39±7.17
GHRH-A	46.11±3.26	64.96±5.51	91.40±9.30
EDV, mL			
Placebo	80.54±3.54	106.10±7.41	139.80±7.47
GHRH-A	78.89±3.54	105.65±7.11	141.45±10.96
SV, mL			
Placebo	31.67±2.11	34.43±2.30	51.40±4.67
GHRH-A	32.78±2.44	40.69±3.11	50.05±3.02
Tagging			
Infarcted area			
Placebo	−13.92±1.14	−5.29±0.63	−6.62±1.00
GHRH-A	−12.78±0.71	−5.72±0.94	−6.07±0.48
Margin of infarcted area			
Placebo	−13.47±0.79	−8.78±0.76	−8.52±1.32
GHRH-A	−13.48±0.86	−10.53±1.38	−11.68±1.15
Remote area			
Placebo	−16.51±0.89	−15.31±1.55	−17.79±1.20
GHRH-A	−14.96±0.83	−15.12±1.57	−16.20±1.21
Perfusion			
Infarcted area			
Placebo	4.00±0.26	4.64±0.43	4.63±0.35
GHRH-A	4.62±0.75	5.11±0.44	5.26±0.58
Margin of infarcted area			
Placebo	4.43±0.50	4.67±0.55	4.84±0.67
GHRH-A	3.82±0.27	4.28±0.17	4.21±0.50

Infarcted area (scar ≥50% of the respective segment), margin of infarcted area (scar <50% of the respective segment), and remote area (remote segments to the infarction area). CMR indicates cardiac magnetic resonance; EDV, end-systolic pressure; ESV, end-systolic volume; GHRH-A, growth hormone–releasing hormone agonist; MI, myocardial infarction; SV, stroke volume.

each group. Five areas of each slide were photographed under light microscopy (Leica Microsystems Inc) at ×10 magnification (100 μm) and blindly analyzed. The total number of positively stained vessels from each sample was quantified and expressed as the average total count per slide with the use of a custom research package (Image J). Image acquisitions were performed with a digital microscope (VisionTek).

Immunostaining

Myocardial sections from border zones of the infarct area were deparaffinized through a series of xylenes and graded alcohol as previously described[20] and stained for phospho-S10 of histone H_3 (pH_3; Abcam, ab5176), active caspase-3 (AF835; R&D), and tropomyosin or troponin T (Abcam, ab17784 or ab8295) as cardiac marker. Nuclei were counterstained with 4′,6-diamidino-2-phenylindole dye (DAPI; Invitrogen); to confirm that the labeling observed was due to binding of the secondary antibody to the primary antibody, we excluded the primary antibodies on parallel sections and used them as negative controls.

All representative images were obtained with fluorescent (Olympus IX81) or a confocal microscopy (LSM710; Zeiss). The total numbers of pH_3- and caspase-3–positive cells were quantified per slide to calculate the numbers of cells per unit area (mm^2) on each sample (n=3 for each pig). Subsequent slides from the same sections (~3 μm apart) stained for Masson's trichrome were scanned (Path Scan Enabler IV; Meyer Instruments) and used to determine the area of each

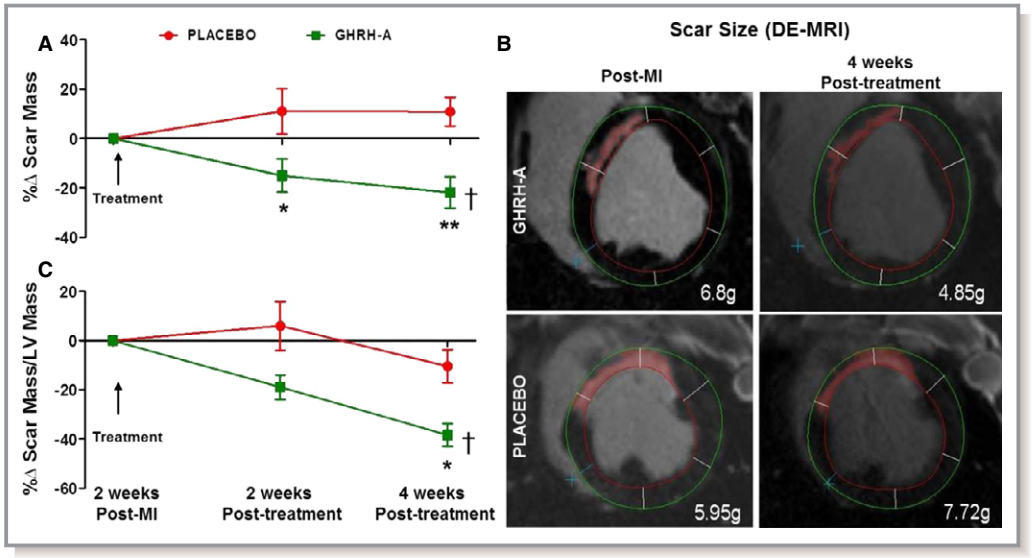

Figure 2. GHRH-A treatment reduces scar mass. A, Percent change of scar mass in GHRH-A group versus placebo group at 2 and 4 weeks post initiation of treatment (2-way ANOVA, between group: **P*=0.04 and ***P*=0.003 vs placebo, respectively). One-way ANOVA: †*P*=0.02 for GHRH-A group. B, Images of hearts from an animal in each group before and 4 weeks after the initiation of treatment. C, Percent change of scar as a percentage of left ventricular mass in GHRH-A group versus placebo group at 2 and 4 weeks postinitiation of treatment (2-way ANOVA, between group: *P*=NS and **P*=0.02 vs placebo, respectively). One-way ANOVA: †*P*=0.0002 for GHRH-A group. GHRH-A indicates growth hormone–releasing hormone agonist.

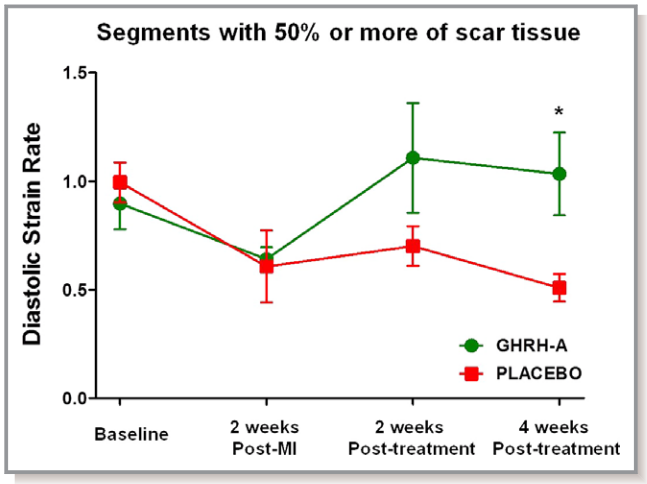

Figure 3. Peak diastolic strain rate improves after GHRH-A treatment. Diastolic strain rate in segments with 50% or more of scar tissue improved in the GHRH-A group but not in placebo group at 4 weeks postinitiation of treatment (2-way ANOVA between-group; Tukey's multiple-comparisons test **P*=0.04). GHRH-A indicates growth hormone–releasing hormone agonist.

sample (1 mm=288 pixels) by using Adobe Photoshop CS3 extended (Adobe).

Statistical Analysis

All data are presented as a mean±SEM. GraphPad Prism (Version 6.0) was used to analyze all data and plot graphs. Comparisons between groups employed the Wilcoxon rank test or Mann–Whitney tests or *t* tests, as appropriate. Variables measured at multiple time points were analyzed by using 1-way ANOVA (for within-group effects) or 2-way ANOVA that included terms for group, time, and group×–time interactions (between-group effects). ANOVA results were further analyzed by post hoc analyses by using either Bonferroni, Tukey, or Dunn multiple-comparison testing. A value of $P<0.05$ was considered statistically significant.

Results

A total of 21 Yorkshire swine were infarcted as described. Nine animals died during surgery due to a cardiac arrest caused by large transmural infarction, and they did not respond to external defibrillation (42.8% mortality). The 12 survivors had no adverse events during the infarction procedure. These animals were randomized into 2 different groups: GHRH-A (MR-409) and placebo. Two weeks post MI, both groups had a similar scar size (Table 3).

Blood Analysis and Body Weight Growth Post GHRH-A Treatment

The animals from the GHRH-A–treated and placebo groups showed identical patterns in serum hematology, chemistry, and cardiac enzymes during the study and exhibited

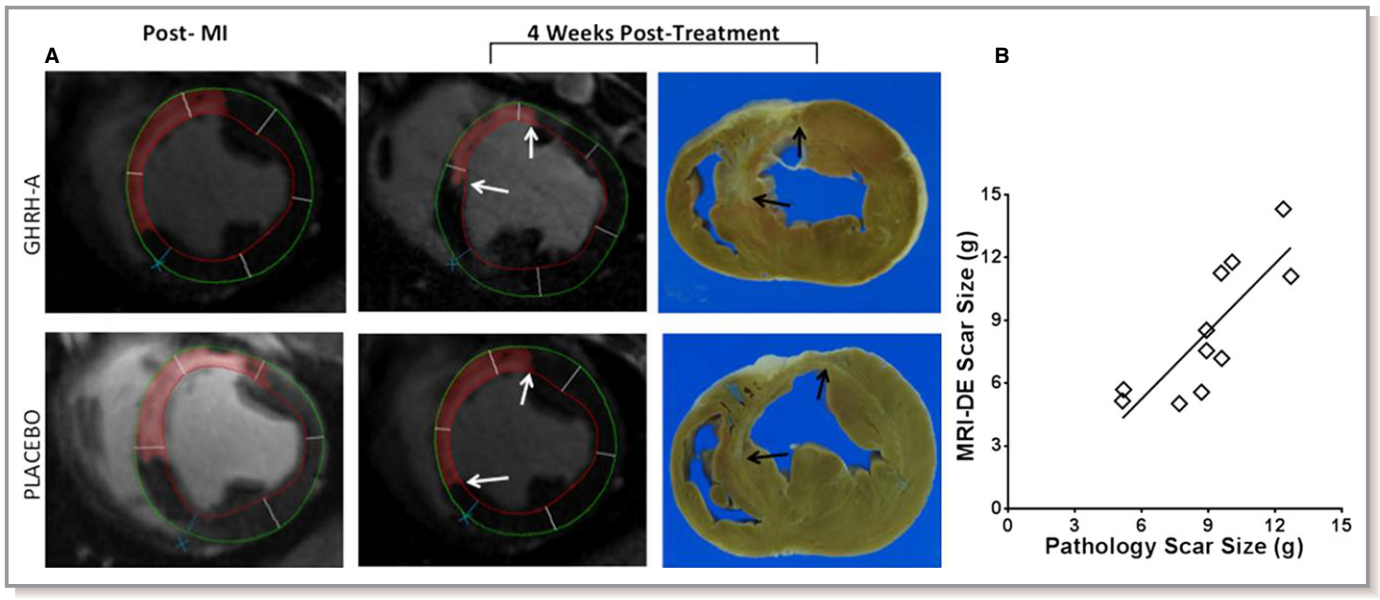

Figure 4. Scar size quantification by gross pathology. A, Representative CMR and gross pathology images of swine hearts in transverse axis from placebo and GHRH-A groups—at post MI and 4 weeks post-treatment time points. Extent of scar size at 4 weeks posttreatment, measured by delayed enhancement and gross pathology, is demarcated by white and black arrows, respectively. B, Scar size as measured by CMR delayed enhancement strongly correlates with gross pathology scar size quantification (Pearson correlation coefficient r=0.82, P=0.002). GHRH-A indicates growth hormone–releasing hormone agonist.

Table 8. Histological Findings Represented by the Relation Between the Numbers of Samples Analyzed and Total Animals in Each Group

		Calcification			Inflammatory Cells		
		Yes			Yes		
	Cells Within Fibrosis	Foci	Granulomatous	No	Sparse	Nodular	Vasculitis
Placebo	6/6	1/6	3/6	2/6	6/6	0/6	0/6
GHRH-A	6/6	1/6	5/6	0/6	5/6	1/6	0/6

GHRH-A indicates growth hormone–releasing hormone agonist.

no evidence of clinically relevant or unexpected laboratory abnormalities (data not shown). Of particular interest were the relative similarities (rise and fall) of enzymes (Table 4) within both groups. The specific cardiac enzymes (creatine kinase–MB and troponin I) are shown in Figure 1. As illustrated in Table 3, no differences in body weight (swine mass) were detected between groups during the study.

Left Ventricular Structural and Functional Changes After GHRH-A Treatment

Although the hemodynamic parameters (Tables 5 and 6), CMR CINE images, contractility index by tagging, and perfusion by CMR (Table 7) revealed similar degrees of global cardiac functional levels in both groups after treatment, the scar mass (Figure 2A and 2B) exhibited substantial reduction in the GHRH-A group (1-way ANOVA, within group: P=0.02) compared with the placebo group after 4 weeks of treatment (2-way ANOVA, between group: P=0.003). Similarly, the scar size as a percentage of LV mass (Figure 2C) was reduced in the GHRH-A group (1-way ANOVA, within group: P=0.0002) compared with the placebo group (2-way ANOVA, between group: P=0.02). Furthermore, the peak diastolic strain rate (Figure 3) in the transmural infarction segments (scar ≥50% of the respective segment) improved after 4 weeks of GHRH-A treatment but not in the placebo group (1.03±0.19 versus 0.51±0.06, respectively, 2-way ANOVA between-group; Tukey`s multiple-comparisons test: P=0.04). Scar size was also quantified based on transverse heart sections from gross pathology. When compared with the CMR delayed enhancement scar

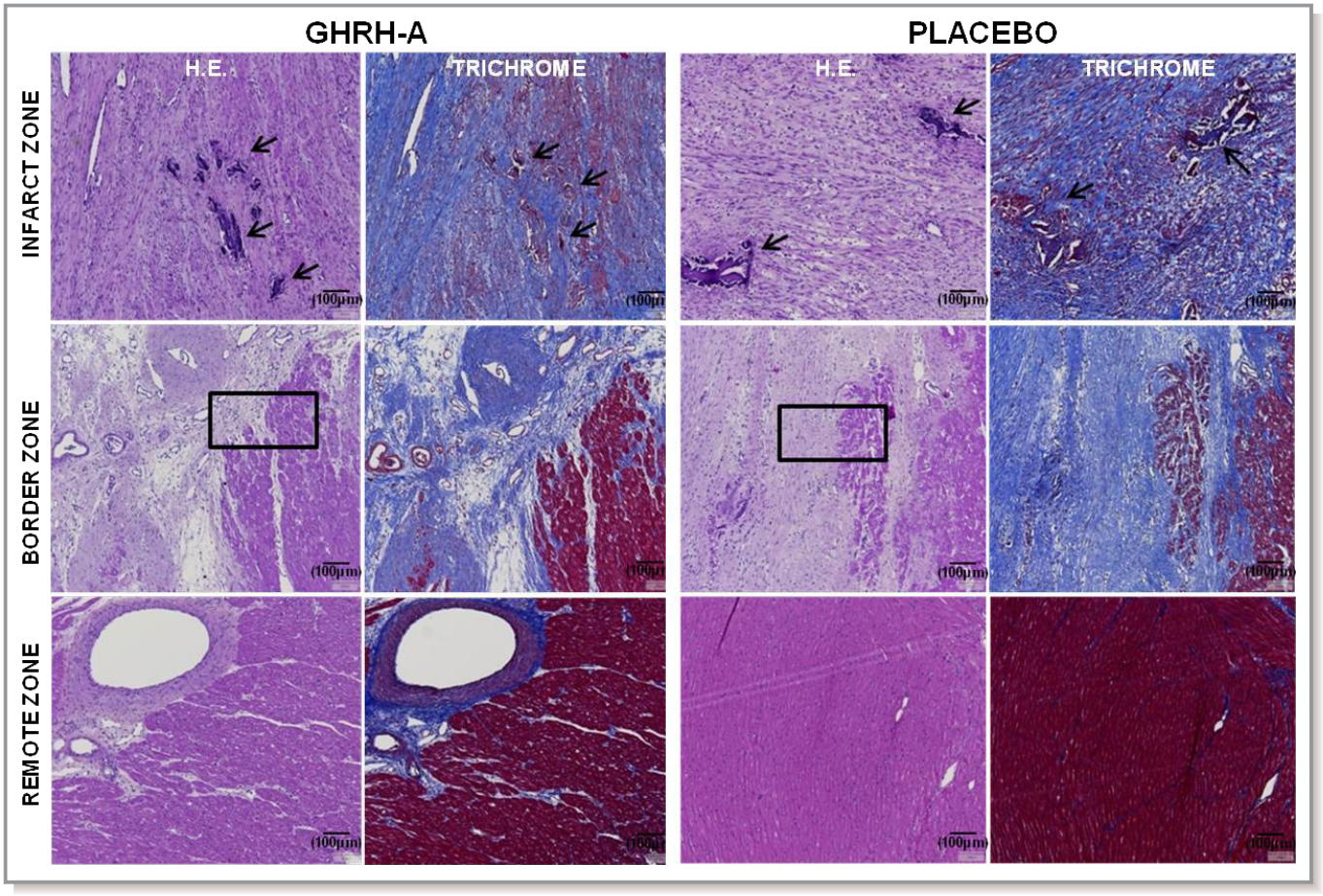

Figure 5. Hematoxylin and eosin– and Masson's trichrome–stained images from GHRH-A and placebo groups. The treated and placebo groups exhibited calcium in the infarct zone (black arrows), evidence of healing fibrosis, and normal myocardium in the border zone (black box), and normal myocardium and vessels in the remote zone. All images at ×10 magnification. Scale bars: 100 μm. GHRH-A indicates growth hormone–releasing hormone agonist.

measurements, there was a strong correlation between the 2 methods, as previously shown[21,22] (Figure 4).

Effect of GHRH-A on the Heart and Other Tissues

In addition to metrics of cardiac function, the histopathologic, gross, and microscopic studies on *ex vivo* tissue samples were performed post-mortem. There was no evidence of tumor formation in any organ analyzed (eg, brain, liver, spleen, kidney, lung, ileum, and pituitary gland) from either the GHRH-A or placebo groups (data not shown). Moreover, the heart weight/ body weight index did not differ between the groups after 4 weeks of treatment (Table 3). Histologically, both groups showed evidence of healing fibrosis, normal myocardium, and the presence of calcium and inflammatory cells related to the calcium deposition. These histological findings are summarized in Table 8, and representative hematoxylin and eosin and Masson's trichrome images from each group are shown in Figure 5.

Increase in GHRHR Expression in the Heart After GHRH-A Treatment

Immunohistochemical staining for GHRHR in the swine hearts (Figure 6A) revealed abundant receptors in cardiac tissue. GHRHRs were more abundant in the border zones compared with their infarct zones in both GHRH-A and placebo groups (73.5±8.1 versus 204.2±4.5 and 105.2±10.9 versus 196.3±2.3, respectively; $P<0.0001$ for both by Kruskal–Wallis test) (Figure 6B), and the GHRH-A group showed a trend toward higher levels in the border zones ($P<0.0625$ versus placebo by Wilcoxon rank test) than did the placebo group (Figure 6C).

Effect of GHRH-A on Vasculogenesis, Cell Proliferation, and Apoptosis

When border zones from heart LV walls were assessed for vascular density (Figure 7), no differences were observed between GHRH-A and placebo (80.28±11.48 versus

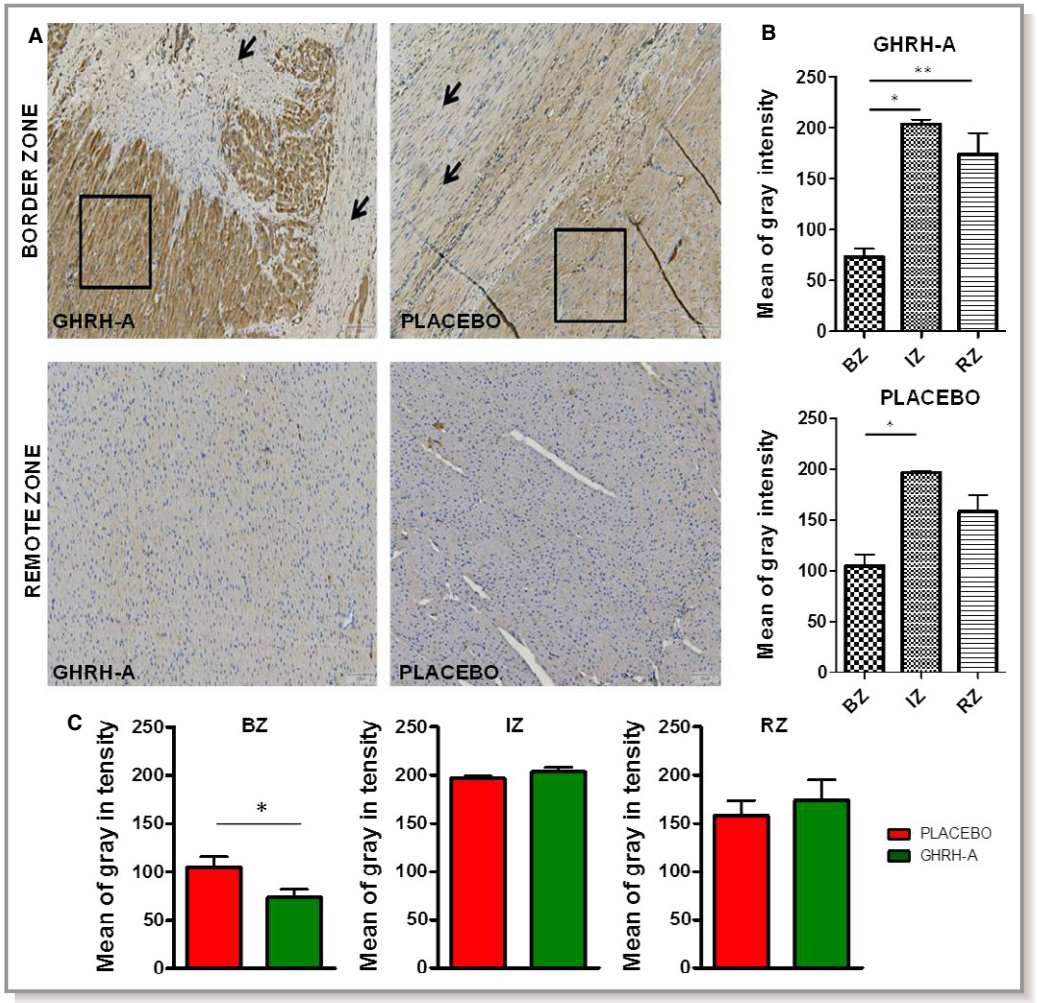

Figure 6. GHRHR expression. A, Example of GHRHR expression (brown color) in the border zones (top) and the remote zone (bottom) in the GHRH-A and placebo groups by immunohistochemical analysis. B, Gray color intensity is inversely proportional to the presence of GHRHR (ie, low gray color intensity corresponds to greater GHRHR expression). GHRHRs were more abundant in the border zones compared with their infarct zones in both GHRH-A and placebo groups (**P*<0.01), as well as more receptor abundance in the border zones compared with its remote zones (***P*<0.01) only in the GHRH-A group by nonparametric test (Kruskal–Wallis) with Dunn's multiple comparison test. C, Comparison between groups demonstrated a tendency towards higher levels of receptors in the border zone of the GHRH-A group versus placebo (**P*<0.0625 by Wilcoxon rank test). GHRH-A indicates growth hormone–releasing hormone agonist; GHRHR, GHRH receptor; BZ, border zone; IZ, infarct zone; RZ, remote zone.

82.58±7.76, respectively; *P*=NS by Mann–Whitney test). Quantification of pH_3- and caspase-3–positive cells (Figure 8A and 8B, respectively) in LV wall border zones demonstrated no difference in the degree of cardiomyocyte proliferation and apoptosis between groups (*P*=NS by Mann–Whitney test). Further, apoptotic activities of noncardiomyocytes (Figure 8C) in the 2 groups were similar (*P*=NS by Mann–Whitney test).

Discussion

The major new findings of this work are that therapy with a potent GHRH agonist has the ability to substantially reduce infarct size and improve diastolic cardiac function in a swine model of subacute cardiomyopathy. These results can be viewed within the broader context of attempt to treat cardiovascular disease through activation of the GH axis. In this regard, there have been several studies that have tested the use of GH to treat cardiac injury. The results of these previous studies on the effects of GH and recombinant GH on rat MI size,[23–26] as well as clinical studies on GH replacement for the failing human heart,[15,16] have been controversial, but GHRH and synthetic GHRH-As provide a potential new beneficial strategy for MI and LV dysfunction.[8,9,11,18,27]

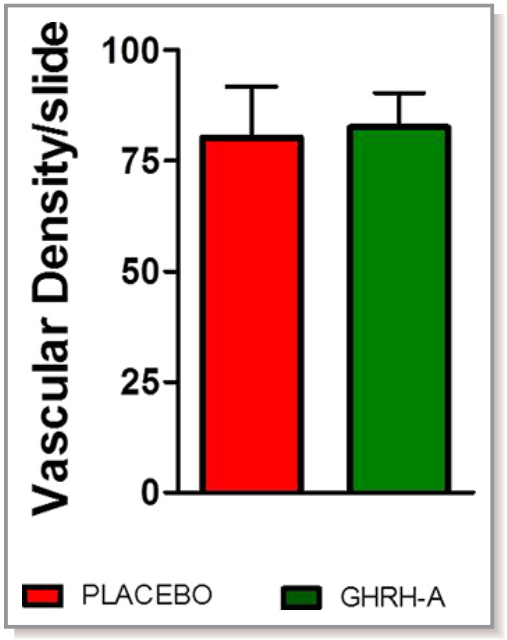

Figure 7. Vascular density assessment in border zones of both GHRH-A and placebo groups. GHRH-A indicates growth hormone–releasing hormone agonist.

We have previously studied in vivo the action of GHRH-A (JI-38 and MR-409) for the treatment of acute and chronic rat MI models.[8,9,18,31] In both models, GHRH-A therapy reduced the degree of cardiac dysfunction and infarct size.[8,9] These findings support the possibility that administration of a GHRH-A, which has higher potency and longer-lasting effects compared with native GHRH,[17,18,28] could have therapeutic benefits in patients with acute MI and chronic ischemic heart disease. This effect was seen following subcutaneous administration of these analogs, twice daily for 4 weeks. Importantly, this treatment regimen did not increase circulating GH and IGF-1 levels. This observation suggests that the benefits were a consequence of local cardiac activation and not regulated by the GH-IGF-1 axis.[9] Based on these results, we performed the first GHRH-A study in a large animal model of reperfusion–ischemia, a preclinical model that recapitulates LV remodeling and therefore is ideal for translation to human application.[19] Here, we report that daily subcutaneous injections of GHRH-A (MR-409) injections (30 $\mu g\ kg^{-1}\ d^{-1}$), using a 4-week regimen in a swine model of subacute ischemic cardiomyopathy, resulted in significantly reduced scar size and improved diastolic LV function.

Reduction of infarct size represents the primary goal of treatment of patients with ST-elevation acute MI.[29] It has been shown that infarct size after ST-elevation acute MI is one of the strongest predictors for LV dysfunction and adverse outcomes compared with other traditional risk parameters.[32,33] Importantly, the development of HF after ST-elevation acute MI has been linked to poorer prognoses.[34] Thus, the attenuation of myocardial fibrosis after GHRH-A therapy represents beneficial changes for the remodeling prevention process and suggests that this treatment would contribute to a prolonged life span, because patients with larger infarcts have greater mortality than those with smaller infarcts.[35] Additionally, the volume of the infarct may be a crucial determinant in the development of arrhythmias related to sudden cardiac death.[36–40] While ischemia leads to both systolic and diastolic dysfunction, previous studies have noted a worse prognosis in patients presenting with diastolic dysfunction.[41] Therefore, we tested the diastolic component of the global cardiac dysfunction. We examined segmental LV diastolic strain rate and found that

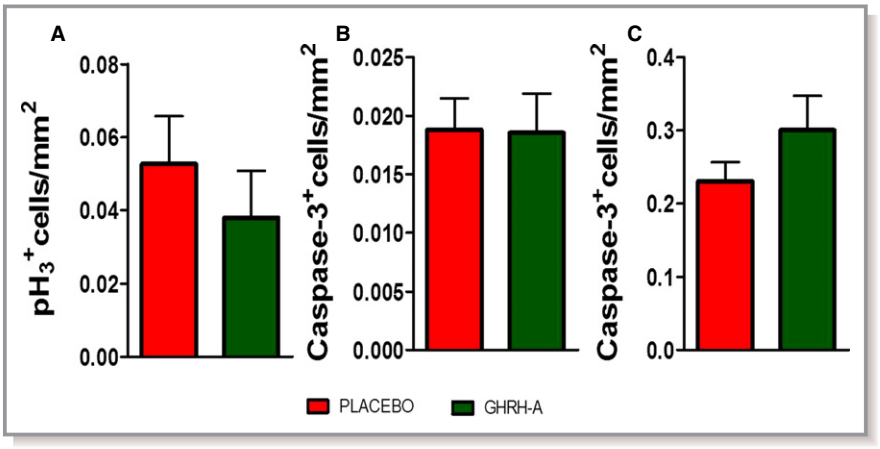

Figure 8. Cardiomyocyte proliferation and apoptosis. A, No differences in cardiomyocyte proliferation was seen between groups in the border zone (*P*=NS by Mann–Whitney test). B, The degree of cardiomyocyte apoptosis found in the border zone was similar in the GHRH-A and placebo groups (*P*=NS by Mann–Whitney test) and (C) similarly for noncardiomyocytes (*P*=NS by Mann–Whitney test). Values are normalized by number of cells per unit area (mm^2). GHRH-A indicates growth hormone–releasing hormone agonist.

administration of this GHRH-A enhanced LV diastolic function. Moreover, after GHRH-A treatment, body weight and heart weight did not change. This corroborates our previous findings in rats in which the administration of a variety of GHRH-As was shown to act locally without causing any adverse effects, such as cardiac hypertrophy, on the process of LV remodeling.[8,9] In contrast, recombinant GH[8] and GH[23] treatments after acute MI increased body and height weight but did not prevent cardiac remodeling.

Surprisingly, our current immunostaining data show that the antifibrotic effect observed in the GHRH-A group was not followed by an increase in vascular density, cardiomyocyte mitosis, or antiapoptotic activity; however, the interpretation of these results needs to be carefully analyzed along with our study limitations. The healing process after an MI in the rodent model differs significantly from the swine model. Therefore, the effects of GHRHA therapy on tissue repair events such as endothelial and cardiomyocyte mitogenesis or apoptosis may occur during early or late stages not covered by our study design.

Our hemodynamic findings were not conclusive regarding potential beneficial effects of GHRH-A on cardiac performance or loading conditions. Importantly, improvements in ejection fraction or hemodynamic parameters were not detected on hemodynamic catheterization in this study. Many of these parameters could be critically affected by intraoperative conditions and/or animal variability. In addition, cardiac structure and function as assessed on CMR images were similar in the 2 groups. This finding suggests that at the dose and dosing regimen used, the primary effect was on scar reduction, which also translated into improved diastolic performance. Although reduction in MI size was the predominant effect, these findings still suggest that this approach has merit and longer-term evaluation outcomes or different dosing regimens should be explored to identify improvements in this animal model.

In agreement with previous studies that showed the presence of GHRHRs on rat cardiomyocytes[8,11] and CSCs,[12] we found GHRHRs in swine cardiac tissue. The border zone of the GHRH-A–treated group exhibited the highest levels of GHRHRs compared with the placebo group and other zones of the heart. These findings suggest that GHRH-A acts through the GHRHR signal transduction pathway in the heart while not dependent on the activation of GH/IGF-1 axis.[8,9,11]

Our current knowledge on the role of GHRH signaling in the heart is still limited; however, GHRH was found to elicit cardioprotective effects on adult rat cardiomyocytes and in the H9c2 cardiac cell line,[11] and these effects required extracellular signal-regulated kinases 1 and 2 (ERK1/2) and phosphatidylinositol-3-kinase/Akt (PI3K/Akt) activation as well as adenylyl cyclase/cyclic AMP/protein kinase A signaling.[11] Penna et al[42] reported that GHRH induces cardioprotection after ischemia–reperfusion injury in isolated rat hearts via activation of reperfusion injury salvage kinase (RISK) and survivor activating factor enhancement (SAFE) pathways through receptor-mediated mechanisms. More recently, our group has demonstrated that agonists of GHRH directly stimulate self-renewal of porcine CSCs and promote their survival in vitro.[12] In addition, inhibitors of ERK and AKT pathways completely abolished the effect of GHRH agonists on CSC proliferation. Because we have not investigated the effect of GHRH on CSCs in vivo, we cannot rule out that the beneficial effect observed in our study is due to stimulation of endogenous CSCs.

Study Limitations

The results of the present study are encouraging, but it is important to note that the pharmacokinetics of the agonist was not fully characterized. Moreover, the dose–response of the GHRH analog was not tested, and this should be studied in the near future to examine whether a higher or earlier (immediately after MI) administration dose of GHRH-A is more efficacious in restoring global cardiac function, because our experimental work did not translate into an improved cardiac performance as was shown in the rat study.[8,9,18] Although only 12 of 21 swine survived the infarct procedure, we believe that the results from the surviving swine could be generalizable as the mortalities noted were all perioperatively related and not due to “healthier” versus “nonhealthier” animals. Hemodynamic parameters between the 2 groups were not different at baseline, corroborating this concept. Further, the individual swine have slight variations in cardiac anatomy, which is an important factor when considering survival of the infarction procedure.

Conclusion

The results of this study suggest that daily subcutaneous administration of GHRH-A is safe, promotes substantial reduction of infarct size, and enhances diastolic function. Further, to more precisely extrapolate the expected effects on humans, studies with longer follow-up (>8 weeks) in a chronic ischemia porcine model and earlier or higher doses of GHRH-A should be performed. Together, these findings provide insight into a potentially new and promising strategy to reduce scar burden after MI and could be beneficial to a large patient population with unmet needs.

Sources of Funding

This work was supported by National Institutes of Health (NIH) R01 grants HL107110, HL084275, and HL094848 and by the

National Heart, Lung, and Blood Institute (all to Dr Hare). Dr Hare is also supported by NIH grant UM1 HL113460 and a grant from the Starr Foundation. Dr Schally is supported by the Medical Research Service of the Department of Veterans Affairs, the South Florida Veterans Affairs Foundation for Research and Education, and the Division of Hematology/Oncology, Department of Pathology and Medicine, Miller School of Medicine, University of Miami. Dr Schally was also supported by the Wallace H. Coulter Foundation SB26MT66142E for the development of GHRH agonists for translation research. Dr Karantalis is supported by an award from the American Heart Association.

Disclosures

Dr Joshua Hare, Dr Norman Block, and Peter Goldstein own equity in Biscayne Pharmaceuticals, licensee of intellectual property used in this study. Biscayne Pharmaceuticals did not provide funding for this study.

References

1. Mozaffarian D, Benjamin EJ, Go AS, Arnett DK, Blaha MJ, Cushman M, de Ferranti S, Despres J, Fullerton HJ, Howard VJ, Huffman MD, Judd SE, Kissela BM, Lackland DT, Lichtman JH, Lisabeth LD, Liu S, Mackey RH, Matchar DB, McGuire DK, Mohler ER III, Moy CS, Muntner P, Mussolino ME, Nasir K, Neumar RW, Nichol G, Palaniappan L, Pandey DK, Reeves MJ, Rodriguez CJ, Sorlie PD, Stein J, Twofighi A, Turan TN, Virani SS, Willey JZ, Woo D, Yeh RW, Turner MB, American Heart Association Statistics Committee and Stroke Statistics Subcommittee. Heart disease and stroke statistics–2014 update: a report from the American Heart Association. *Circulation*. 2014;129:e28–e292.
2. Joffe SW, Webster K, McManus DD, Kiernan MS, Lessard D, Yarzebski J, Darling C, Gore JM, Goldberg RJ. Improved survival after heart failure: a community-based perspective. *J Am Heart Assoc*. 2013;2:e000053 doi: 10.1161/JAHA.113.000053.
3. Sacca L. Heart failure as a multiple hormonal deficiency syndrome. *Circ Heart Fail*. 2009;2:151–156.
4. Suncion VY, Ghersin E, Fishman JE, Zambrano JP, Karantalis V, Mandel N, Nelson KH, Gerstenblith G, Difede Velazquez DL, Breton E, Sitammagari K, Schulman IH, Taldone SN, Williams AR, Sanina C, Johnston PV, Brinker J, Altman P, Mushtaq M, Trachtenberg B, Mendizabal AM, Tracy M, Da Silva J, McNiece IK, Lardo AC, George RT, Hare JM, Heldman AW. Does transendocardial injection of mesenchymal stem cells improve myocardial function locally or globally? An analysis from the Percutaneous Stem Cell Injection Delivery Effects on Neomyogenesis (POSEIDON) randomized trial. *Circ Res*. 2014;114:1292–1301.
5. Karantalis V, DiFede DL, Gerstenblith G, Pham S, Symes J, Zambrano JP, Fishman J, Pattany P, McNiece I, Conte J, Schulman S, Wu K, Shah A, Breton E, Davis-Sproul J, Schwarz R, Feigenbaum G, Mushtaq M, Suncion VY, Lardo AC, Borrello I, Mendizabal A, Karas TZ, Byrnes J, Lowery M, Heldman AW, Hare JM. Autologous mesenchymal stem cells produce concordant improvements in regional function, tissue perfusion, and fibrotic burden when administered to patients undergoing coronary artery bypass grafting: the prospective randomized study of mesenchymal stem cell therapy in patients undergoing cardiac surgery (PROMETHEUS) trial. *Circ Res*. 2014;114:1302–1310.
6. Heldman AW, DiFede DL, Fishman JE, Zambrano JP, Trachtenberg BH, Karantalis V, Mushtaq M, Williams AR, Suncion VY, McNiece IK, Ghersin E, Soto V, Lopera G, Miki R, Willens H, Hendel R, Mitrani R, Pattany P, Feigenbaum G, Oskouei B, Byrnes J, Lowery MH, Sierra J, Pujol MV, Delgado C, Gonzalez PJ, Rodriguez JE, Bagno LL, Rouy D, Altman P, Foo CW, da Silva J, Anderson E, Schwarz R, Mendizabal A, Hare JM. Transendocardial mesenchymal stem cells and mononuclear bone marrow cells for ischemic cardiomyopathy: the TAC-HFT randomized trial. *JAMA*. 2014;311:62–73.
7. Kanashiro-Takeuchi RM, Schulman IH, Hare JM. Pharmacologic and genetic strategies to enhance cell therapy for cardiac regeneration. *J Mol Cell Cardiol*. 2011;51:619–625.
8. Kanashiro-Takeuchi RM, Tziomalos K, Takeuchi LM, Treuer AV, Lamirault G, Dulce R, Hurtado M, Song Y, Block NL, Rick F, Klukovits A, Hu Q, Varga JL, Schally AV, Hare JM. Cardioprotective effects of growth hormone-releasing hormone agonist after myocardial infarction. *Proc Natl Acad Sci USA*. 2010;107:2604–2609.
9. Kanashiro-Takeuchi RM, Takeuchi LM, Rick FG, Dulce R, Treuer AV, Florea V, Rodrigues CO, Paulino EC, Hatzistergos KE, Selem SM, Gonzalez DR, Block NL, Schally AV, Hare JM. Activation of growth hormone releasing hormone (GHRH) receptor stimulates cardiac reverse remodeling after myocardial infarction (MI). *Proc Natl Acad Sci USA*. 2012;109:559–563.
10. Cittadini A, Marra AM, Arcopinto M, Bobbio E, Salzano A, Sirico D, Napoli R, Colao A, Longobardi S, Baliga RR, Bossone E, Sacca L. Growth hormone replacement delays the progression of chronic heart failure combined with growth hormone deficiency: an extension of a randomized controlled single-blind study. *JACC Heart Fail*. 2013;1:325–330.
11. Granata R, Trovato L, Gallo MP, Destefanis S, Settanni F, Scarlatti F, Brero A, Ramella R, Volante M, Isgaard J, Levi R, Papotti M, Alloatti G, Ghigo E. Growth hormone-releasing hormone promotes survival of cardiac myocytes in vitro and protects against ischaemia-reperfusion injury in rat heart. *Cardiovasc Res*. 2009;83:303–312.
12. Florea V, Majid SS, Kanashiro-Takeuchi RM, Cai RZ, Block NL, Schally AV, Hare JM, Rodrigues CO. Agonists of growth hormone-releasing hormone stimulate self-renewal of cardiac stem cells and promote their survival. *Proc Natl Acad Sci USA*. 2014;111:17260–17265.
13. Aimaretti G, Baldelli R, Corneli G, Bellone S, Rovere S, Croce C, Ragazzoni F, Giordano R, Arvat E, Bona G, Ghigo E. GHRH and GH secretagogues: clinical perspectives and safety. *Pediatr Endocrinol Rev*. 2004;2(Suppl 1):86–92.
14. Kiaris H, Schally AV, Kalofoutis A. Extrapituitary effects of the growth hormone-releasing hormone. *Vitam Horm*. 2005;70:1–24.
15. Fazio S, Sabatini D, Capaldo B, Vigorito C, Giordano A, Guida R, Pardo F, Biondi B, Sacca L. A preliminary study of growth hormone in the treatment of dilated cardiomyopathy. *N Engl J Med*. 1996;334:809–814.
16. Osterziel KJ, Strohm O, Schuler J, Friedrich M, Hanlein D, Willenbrock R, Anker SD, Poole-Wilson PA, Ranke MB, Dietz R. Randomised, double-blind, placebo-controlled trial of human recombinant growth hormone in patients with chronic heart failure due to dilated cardiomyopathy. *Lancet*. 1998;351:1233–1237.
17. Izdebski J, Pinski J, Horvath JE, Halmos G, Groot K, Schally AV. Synthesis and biological evaluation of superactive agonists of growth hormone-releasing hormone. *Proc Natl Acad Sci USA*. 1995;92:4872–4876.
18. Cai R, Schally AV, Cui T, Szalontay L, Halmos G, Sha W, Kovacs M, Jaszberenyi M, He J, Rick FG, Popovics P, Kanashiro-Takeuchi R, Hare JM, Block NL, Zarandi M. Synthesis of new potent agonistic analogs of growth hormone-releasing hormone (GHRH) and evaluation of their endocrine and cardiac activities. *Peptides*. 2014;52:104–112.
19. McCall FC, Telukuntla KS, Karantalis V, Suncion VY, Heldman AW, Mushtaq M, Williams AR, Hare JM. Myocardial infarction and intramyocardial injection models in swine. *Nat Protoc*. 2012;7:1479–1496.
20. Hatzistergos KE, Quevedo H, Oskouei BN, Hu Q, Feigenbaum GS, Margitich IS, Mazhari R, Boyle AJ, Zambrano JP, Rodriguez JE, Dulce R, Pattany PM, Valdes D, Revilla C, Heldman AW, McNiece I, Hare JM. Bone marrow mesenchymal stem cells stimulate cardiac stem cell proliferation and differentiation. *Circ Res*. 2010;107:913–922.
21. Dash R, Chung J, Ikeno F, Hahn-Windgassen A, Matsuura Y, Bennett MV, Lyons JK, Teramoto T, Robbins RC, McConnell MV, Yeung AC, Brinton TJ, Harnish PP, Yang PC. Dual manganese-enhanced and delayed gadolinium-enhanced MRI detects myocardial border zone injury in a pig ischemia-reperfusion model. *Circ Cardiovasc Imaging*. 2011;4:574–582.
22. Kim RJ, Chen EL, Lima JA, Judd RM. Myocardial GD-DTPA kinetics determine MRI contrast enhancement and reflect the extent and severity of myocardial injury after acute reperfused infarction. *Circulation*. 1996;94:3318–3326.
23. Mill JG, Zornoff LA, Okoshi MP, Okoshi K, Padovani CR, Sugisaki M, Leite CM, Cicogna AC. The early administration of growth hormone results in deleterious effects on ventricular remodeling after acute myocardial infarction. *Arq Bras Cardiol*. 2005;84:115–121.
24. Laguens RP, Castagnino HE, Jorg ME, Hamamura S. Reduced injury and scar in acute myocardial infarctions treated with human growth hormone. *Jpn Heart J*. 1998;39:809–817.
25. Jin H, Yang R, Lu H, Ogasawara AK, Li W, Ryan A, Peale F, Paoni NF. Effects of early treatment with growth hormone on infarct size, survival, and cardiac gene expression after acute myocardial infarction. *Growth Horm IGF Res*. 2002;12:208–215.
26. Hatzistergos KE, Mitsi AC, Zachariou C, Skyrlas A, Kapatou E, Agelaki MG, Fotopoulos A, Kolettis TM, Malamou-Mitsi V. Randomised comparison of growth hormone versus IGF-1 on early post-myocardial infarction ventricular remodelling in rats. *Growth Horm IGF Res*. 2008;18:157–165.

27. MacAndrew JT, Ellery SS, Parry MA, Pan LC, Black SC. Efficacy of a growth hormone-releasing peptide mimetic in cardiac ischemia/reperfusion injury. *Eur J Pharmacol*. 2001;432:195–202.
28. Dubreuil P, Brazeau P, Moreau S, Farmer C, Coy D, Abribat T. The use of pigs as an animal model to evaluate the efficacy, potency and specificity of two growth hormone releasing factor analogues. *Growth Horm IGF Res*. 2001;11:173–186.
29. Mewton N, Elbaz M, Piot C, Ovize M. Infarct size reduction in patients with STEMI: why we can do it!. *J Cardiovasc Pharmacol Ther*. 2011;16:298–303.
30. Kim RJ, Fieno DS, Parrish TB, Harris K, Chen EL, Simonetti O, Bundy J, Finn JP, Klocke FJ, Judd RM. Relationship of MRI delayed contrast enhancement to irreversible injury, infarct age, and contractile function. *Circulation*. 1999;100:1992–2002.
31. Kanashiro-Takeuchi R, Szalontay L, Schally A, Takeuchi L, Popovics P, Jaszberenyi M, Vidaurre I, Zarandi M, Cai R, Block N, Hare J, Rick F. (2015). New therapeutic approach to heart failure due to myocardial infarction based on targeting growth hormone-releasing hormone receptor. *Oncotarget,* 5. Retrieved from http://www.impactjournals.com/oncotarget/index.php?journal=oncotarget&page=article&op=view&path%5B%5D=3303.
32. Larose E, Rodes-Cabau J, Pibarot P, Rinfret S, Proulx G, Nguyen CM, Dery JP, Gleeton O, Roy L, Noel B, Barbeau G, Rouleau J, Boudreault JR, Amyot M, De Larochelliere R, Bertrand OF. Predicting late myocardial recovery and outcomes in the early hours of ST-segment elevation myocardial infarction traditional measures compared with microvascular obstruction, salvaged myocardium, and necrosis characteristics by cardiovascular magnetic resonance. *J Am Coll Cardiol*. 2010;55:2459–2469.
33. de Waha S, Eitel I, Desch S, Fuernau G, Lurz P, Stiermaier T, Blazek S, Schuler G, Thiele H. Prognosis after ST-elevation myocardial infarction: a study on cardiac magnetic resonance imaging versus clinical routine. *Trials*. 2014;15:249.
34. Morrow DA, Antman EM, Charlesworth A, Cairns R, Murphy SA, de Lemos JA, Giugliano RP, McCabe CH, Braunwald E. TIMI risk score for ST-elevation myocardial infarction: a convenient, bedside, clinical score for risk assessment at presentation: an intravenous NPA for treatment of infarcting myocardium early II trial substudy. *Circulation*. 2000;102:2031–2037.
35. Watanabe E, Abbasi SA, Heydari B, Coelho-Filho OR, Shah R, Neilan TG, Murthy VL, Mongeon FP, Barbhaiya C, Jerosch-Herold M, Blankstein R, Hatabu H, van der Geest RJ, Stevenson WG, Kwong RY. Infarct tissue heterogeneity by contrast-enhanced magnetic resonance imaging is a novel predictor of mortality in patients with chronic coronary artery disease and left ventricular dysfunction. *Circ Cardiovasc Imaging*. 2014;7:887–894.
36. Bello D, Einhorn A, Kaushal R, Kenchaiah S, Raney A, Fieno D, Narula J, Goldberger J, Shivkumar K, Subacius H, Kadish A. Cardiac magnetic resonance imaging: infarct size is an independent predictor of mortality in patients with coronary artery disease. *Magn Reson Imaging*. 2011;29:50–56.
37. Miller TD, Christian TF, Hopfenspirger MR, Hodge DO, Gersh BJ, Gibbons RJ. Infarct size after acute myocardial infarction measured by quantitative tomographic 99mTc sestamibi imaging predicts subsequent mortality. *Circulation*. 1995;92:334–341.
38. Yan AT, Shayne AJ, Brown KA, Gupta SN, Chan CW, Luu TM, Di Carli MF, Reynolds HG, Stevenson WG, Kwong RY. Characterization of the peri-infarct zone by contrast-enhanced cardiac magnetic resonance imaging is a powerful predictor of post-myocardial infarction mortality. *Circulation*. 2006;114:32–39.
39. Wu E, Ortiz JT, Tejedor P, Lee DC, Bucciarelli-Ducci C, Kansal P, Carr JC, Holly TA, Lloyd-Jones D, Klocke FJ, Bonow RO. Infarct size by contrast enhanced cardiac magnetic resonance is a stronger predictor of outcomes than left ventricular ejection fraction or end-systolic volume index: prospective cohort study. *Heart*. 2008;94:730–736.
40. Geltman EM. Infarct size as a determinant of acute and long-term prognosis. *Cardiol Clin*. 1984;2:95–103.
41. Azevedo CF, Amado LC, Kraitchman DL, Gerber BL, Osman NF, Rochitte CE, Edvardsen T, Lima JA. Persistent diastolic dysfunction despite complete systolic functional recovery after reperfused acute myocardial infarction demonstrated by tagged magnetic resonance imaging. *Eur Heart J*. 2004;25:1419–1427.
42. Penna C, Settanni F, Tullio F, Trovato L, Pagliaro P, Alloatti G, Ghigo E, Granata R. GH-releasing hormone induces cardioprotection in isolated male rat heart via activation of risk and safe pathways. *Endocrinology*. 2013;154:1624–1635.